JACS
JOURNAL OF THE AMERICAN CHEMICAL SOCIETY
pubs.acs.org/JACS
Article

Influence of Curvature on the Physical Properties and Reactivity of Triplet Corannulene Nitrene

Kelley S. McKissic,[#] Mrinal Chakraborty,[#] Dmitrii Govorov,[#] Mayukh Majumder, DeAnte F. Judkins,[§] Rajkumar Merugu,[§] H. Dushanee M. Sriyarathne,[§] Anushree Das,[§] W. Dinindu Mendis,[§] Jan-Simon von Glasenapp, Rainer Herges, Christopher M. Hadad, James Mack, Manabu Abe, and Anna D. Gudmundsdottir*

Cite This: https://doi.org/10.1021/jacs.4c07846

ABSTRACT: Although nitrene chemistry is promising for the light-induced modification of organic compounds, the reactivity of large polycyclic aromatic compounds and the effects of their curvature remain unexplored. Irradiation of azidocorannulene (**1**) in methanol/acetonitrile followed by HCl addition produced diastereomers **5** and **5′**. Azirine **2** is apparently trapped by methanol to form diastereomeric acetal derivatives that are hydrolyzed with HCl to yield **5** and **5′**. ESR spectroscopy in a glassy matrix at 77 K showed that irradiation of **1** yields corannulene nitrene ^{3}**1N**, which has significant 1,3-biradical character. Irradiation of **1** in a glassy matrix resulted in a new absorption band in the region of 360−440 nm, with λ_{max} at 360 and 410 nm, attributed to ^{3}**1N**, as supported by time-dependent density function theory calculations, which placed the major electronic transitions of ^{3}**1N** at 367 nm (f = 0.0407) and 440 nm (f = 0.0353). Laser flash photolysis of **1** revealed a similar absorption spectrum. Nitrene ^{3}**1N** had a lifetime of only a few hundred nanoseconds and was efficiently quenched by oxygen, because of its 1,3-biradical character. CASPT2(12,11)/6-311G** calculations revealed small energy gap (7.2 kcal/mol) between singlet and triplet configurations, suggesting that ^{3}**1N** is formed by intersystem crossing of ^{1}**1N** to ^{3}**1N**. Spin-density, nucleus-independent chemical shift, and anisotropy of the induced current density calculations verified that ^{3}**1N** is a triplet vinylnitrene with unpaired electrons localized on the C═C−N moiety; decaying by intersystem crossing to **2**, which is more stable owing to its aromaticity, as supported by calculations (SA-CASSCF/QD-NEVPT2/CBS).

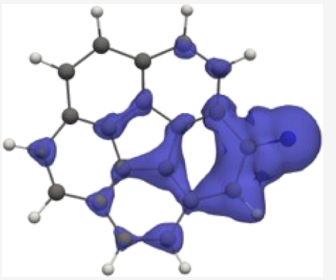

INTRODUCTION

Corannulene ($C_{20}H_{10}$), a polycyclic aromatic hydrocarbon, can be considered as a fragment of buckyball, C_{60}.[1] The corannulene framework is formed by the edge-to-edge fusion of five benzene rings into a loop, resulting in a five-membered core at the center. This arrangement has intrinsic ring strain, which is minimized by adopting a bowl-like structure. The bowl-like shape of corannulene is a fundamental structural feature that sets it apart from other polycyclic aromatic hydrocarbons. Analogous to the well-known umbrella inversion of amines, corannulene undergoes rapid bowl-to-bowl inversion through a fully planar transition state.

In recent years, nonplanar polycyclic aromatic hydrocarbons have been investigated to correlate their structures with their physical properties and reactivity.[2] These efforts have resulted in numerous applications of corannulene derivatives in host−guest chemistry, metal−organic frameworks, porous organic polymers, organic field-effect transistors, and nonlinear optical materials.[2,3] We are interested in investigating the effect of the curved corannulene moiety on the chemistry of corannulene nitrene, as this class of nitrenes has not been examined, despite a growing interest in nitrene chemistry and a better understanding of the physical properties and reactivity of nitrenes over last few decades.[4]

Generally, when exposed to light, organic azides release a nitrogen molecule to form a nitrene intermediate, characterized as a divalent nitrogen-based radical. The reactivity of these nitrene intermediates depends on their substituents and whether they adopt a singlet or triplet configuration. Triplet nitrenes are electron-deficient intermediates that are stabilized by electron-donating groups such as alkyl, vinyl, and phenyl substituents. Most triplet alkyl- and phenylnitrenes are long-lived intermediates that decay by dimerization in solution and are stable at cryogenic temperatures.[5] In contrast, triplet vinylnitrenes are short-lived in solution because they decay by intersystem crossing and are generally unstable at cryogenic temperatures, unless incorporated into a cyclic structure that restricts rotation around the vinylic bond.[6] In contrast, triplet oxycarbonyl-nitrenes have electron-withdrawing substituents and do not decay by dimerization in solution, instead

Received: June 10, 2024
Revised: November 14, 2024
Accepted: November 18, 2024

abstracting a H atom from solvents with abstractable H atoms, such as methanol.[7] Phenylnitrene derivatives have been studied extensively, both in solution and in cryogenic matrices.[8] Generally, direct irradiation of phenyl azide forms the corresponding singlet phenylnitrene. At ambient temperature, singlet phenylnitrene inserts into itself to form an azirine, which reacts further to yield ketenimine derivatives. At cryogenic temperatures, intersystem crossing of the singlet phenylnitrene to its triplet configuration competes with azirine formation. Interestingly, singlet phenylnitrenes with two ortho substituents can insert into local chemical bonds at ambient temperature, but this reaction is indiscriminative and can result in a complex mixture of products.[9]

Owing to this improved understanding of the complex reactivity of nitrene intermediates and their azido precursors as well as the drive for using light as a sustainable reagent, nitrenes have been successfully employed in synthetic applications.[10] Notably, the reactivity of nitrenes during synthetic applications has also been controlled by forming metallonitrenes.[11]

The reactivity of nitrene intermediates incorporated into polycyclic aromatic hydrocarbon offers a novel approach for light-induced modifications, which can be used to tailor the chemical properties of polycyclic aromatic hydrocarbon, rather than relying on bimolecular reactions between polycyclic aromatic hydrocarbons and nitrene molecules.[12] For example, nitrenes formed on the corannulene framework can enable the functionalization of corannulene through the formation of new C−N bonds, using light as the sole driving force. However, the reactivity of large polycyclic aromatic hydrocarbons has not yet been studied.

Herein, we theorized that the curved aromatic surface of triplet corannulene nitrene ^{3}**1N** would influence its reactivity and spectroscopic properties. Compared with triplet arylnitrenes, ^{3}**1N** should have more localized unpaired electrons, resulting in more triplet vinylnitrene-like reactivity. To characterize the reactivity and physical properties of ^{3}**1N**, we conducted product studies, laser flash photolysis at ambient temperature, and absorption and ESR spectroscopic studies in cryogenic matrices of azidocorannulene (**1**). Computations, employed to aid our understanding of the experimental findings, indicated that the unpaired electrons in ^{3}**1N** are mainly localized on the vinylnitrene moiety and that ^{3}**1N** decays to form an azirine (**2**) owing to the steric demand of the curved surface, which is also reflected by its diminished aromaticity.

RESULTS AND DISCUSSION

Product Studies. Photolysis of azidocorannulene (**1**) in an argon-saturated 1:1 mixture of methanol and acetonitrile followed by quenching with HCl led to the formation of 2-amino-substituted hemiacetals (**5** and **5′**, Scheme 1). These products provide evidence for the formation of an azirine intermediate. For flat aromatic systems, the trapping of an arylnitrene-derived azirine with methanol leads to a 2-amino-substituted aryl alcohol,[13] which provides a plausible mechanism for the formation of **5** and **5′**. It should be noted that the final products are not fully aromatic and that the hydrolysis by HCl stops at the hemiacetal stage.

Furthermore, the trapping of azirine **2** with methanol offers a new and mild method for synthesizing substituted dihydrocorannulene. In earlier work, Sygula et al. demonstrated that corannulene can be reacted with organolithium reagents to produce monosubstituted dihydrocorannulene.[14] More recently, Nishibayashi and colleagues showed that corannulene can be functionalized through radical addition, using a photoredox catalyst and silica-substituted amines to generate monosubstituted dihydrocorannulene derivatives.[15] Aryl azirines have also been trapped with nucleophiles. For example, Carroll et al. showed that irradiation of phenyl azide and ethanethiol results in the formation of thioethoxyanline through trapping of phenyl azirine.[16] Levya and Platz demonstrated that irradiation of α-azidonaphthalene and diethylamine at −60 °C yields N^1,N^1-diethylnaphthalene-1,2-diamine.[17] Furthermore, Nay et al. found that irradiation of α-azidonaphthalene and cyclohexyl amine at ambient temperature results in (5*H*-benzo[*c*]azepin-1-yl)-cyclohexylamine.[18]

Scheme 1. Products Obtained by Photolysis of Azidcorannulene 1 in an Acetonitrile/Methanol Mixture

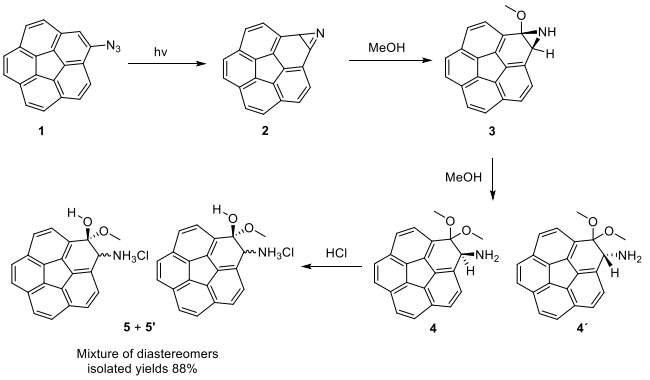

Scheme 2. Possible Pathways for Forming Azirine 2 from Azidocorannulene 1

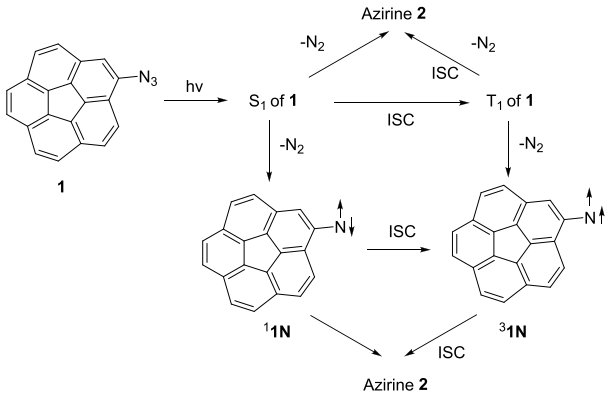

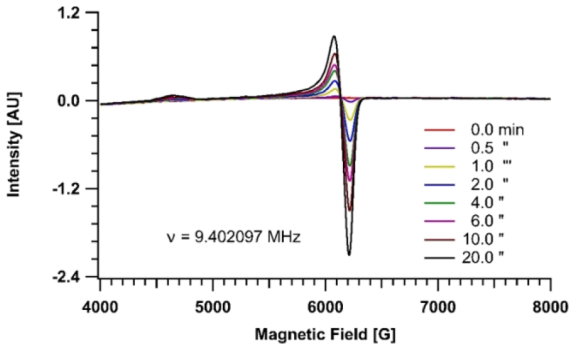

Figure 1. ESR spectra as a function of irradiation time of azidocorannulen **1** at 80 K.

https://doi.org/10.1021/jacs.4c07846
J. Am. Chem. Soc. XXXX, XXX, XXX−XXX

Scheme 3. Measured D/hc Values and Calculated Spin Densities of Various Aryl- and Vinylnitrenes at the B3LYP/6-31+G(d) Level of theory[6a,26b]

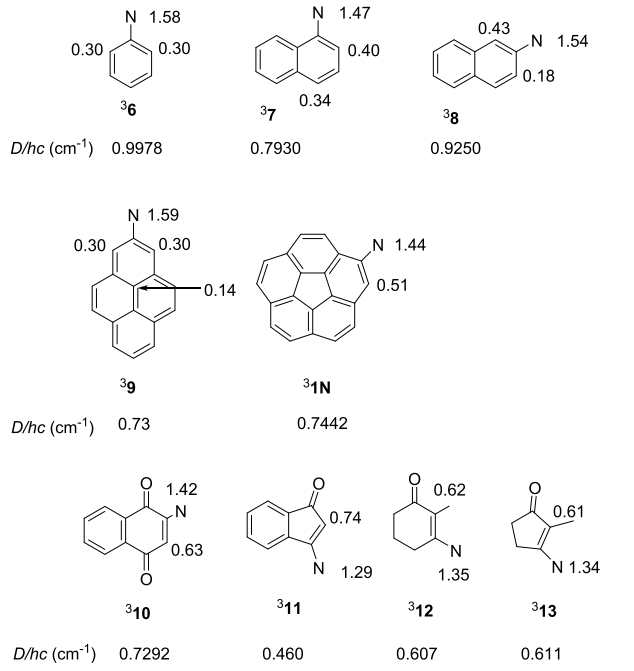

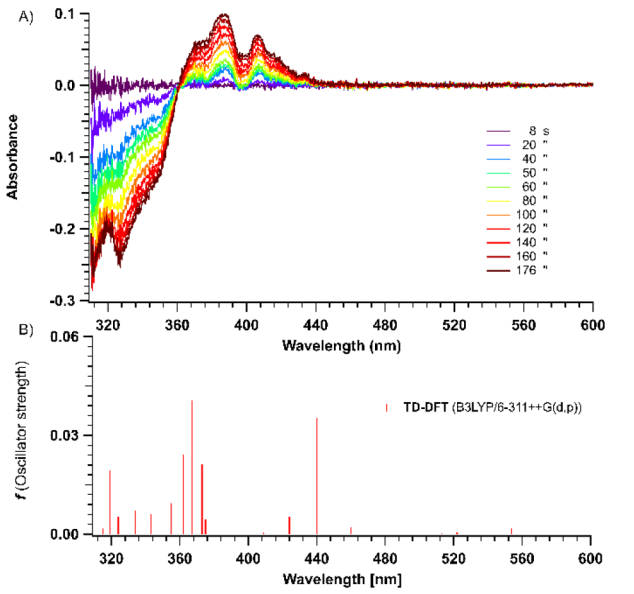

Figure 2. (A) Differential UV absorption spectra obtained upon irradiating azidocorannulene **1** in a glassy matrix at 80 K. (B) TD-DFT (B3LYP/6-311++G(d,p)) calculated electronic transitions for ^{3}**1N**.

Thus, the products generated by nucleophilic trapping of aryl azirines differ from those produced from azirine **2**.

Homodesmic calculations suggest that the aromatic stabilization energy of bowl-shaped corannulene is 10.7 kcal/mol lower than that of planar corannulene, and the inversion barrier has been experimentally estimated to be on the same order.[19] Additionally, owing to the curvature of corannulene, the peripheral carbon atoms experience ring strain. We theorize that complete hydrolysis followed by rearomatization of the hemiacetal would lead to a strained corannulene ring.

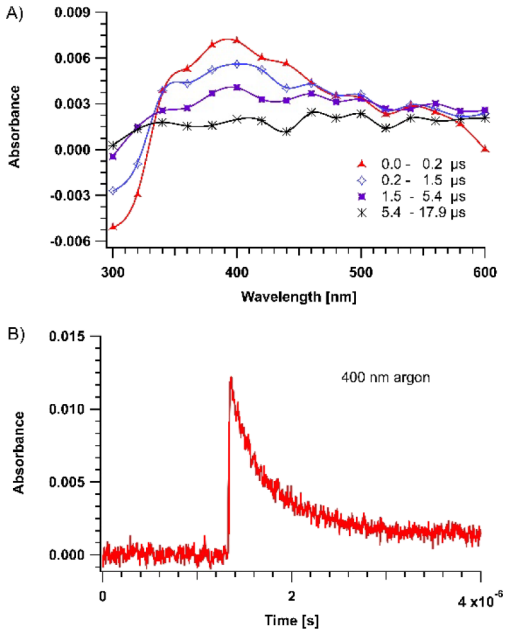

Figure 3. (A) Transient absorption obtained by laser flash photolysis of **1** in argon-saturated acetonitrile. (B) Kinetic trace at 400 nm.

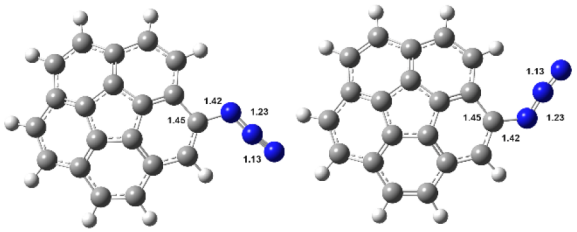

1A (0) kcal/mol **1B** (1.7) kcal/mol

Figure 4. Optimized conformer **1A** and **1B** (B3LYP/6-311++G(d,p)). The numbers are the calculated bond distances in Å.

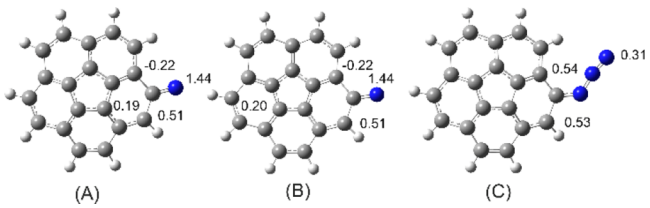

Figure 5. Calculated spin densities for the optimized structures of (A) ^{3}**1N**, (B) the transition state for the inversion of ^{3}**1N**, and (C) T_1 of **1A** at the B3LYP/6-311++G(d,p) level of theory.

Energetically, aromatic stabilization, which is reduced by the curvature of corannulene, is unlikely to compensate for this strain.

Upon irradiation of an argon-saturated toluene-d_8 solution of **1** with a high-pressure mercury arc lamp through a Pyrex filter for 48 h, a polymeric tar was isolated and the starting material was completely depleted. This observation is consistent with previous reports of azirine self-polymerization.[6a]

Although the product studies in argon-saturated solution indicated that the initial photoproduct was corannulene azirine (**2**), they did not reveal the reaction mechanism. Azirine **2**

https://doi.org/10.1021/jacs.4c07846
J. Am. Chem. Soc. XXXX, XXX, XXX−XXX

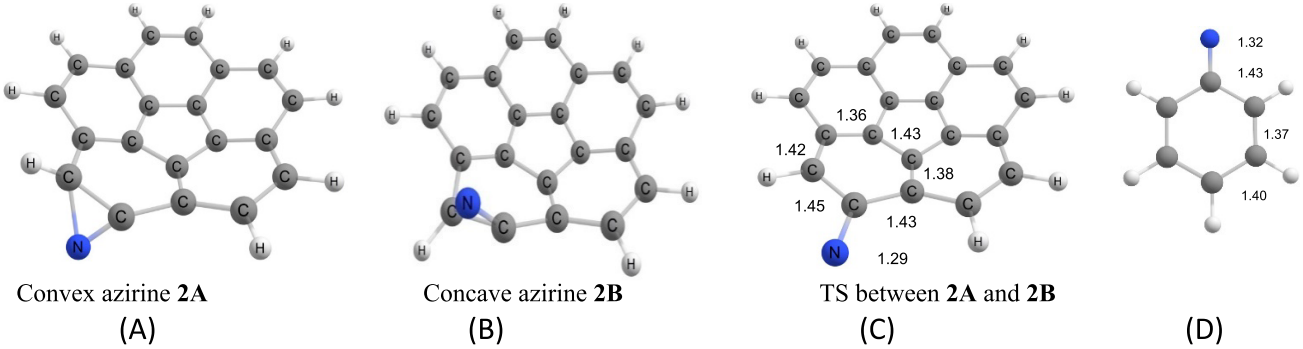

Figure 6. Optimized structures of (A) azirine **2A**, (B) azirine **2B**, and (C) the transition state between **2A** and **2B** and (D) triplet phenylnitrine calculated at the ωB97-X/def2-TZVP level of theory. Numbers are the calculated bond distances in Å.

Table 1. Energy Gaps between Singlet and Triplet Configurations of Nitrenes Calculated at the ωB97-X/def2-TZVP/(CASPT2(12,11)/6-311G(d,p) Level of Theory

nitrene	ΔE_{ST}, kcal/mol
α-pyrene nitrene	6.2
β-pyrene nitrene	9.5
corannulene nitrene ^{3}**1N**	7.2

Table 2. Energy Gaps between Triplet Nitrenes and Corresponding Azirine Products Calculated at the ωB97-X/def2-TZVP Level of Theory

triplet nitrene	Δ*E*, kcal/mol	azirine
α-naphthalene nitrene	10.4	α-naphthalene azirine
β-naphthalene nitrene	27.7	β-naphthalene azirine
α-pyrene nitrene	21.2	α-pyrene azirine
^{3}**1N**	0.3	**2**

Table 3. Energies of ^{3}1N and Azirines 2A and 2B Calculated at the SA-CASSCF/QD-NEVPT2/CBS Level of Theory

compound	*E*, kcal/mol
nitrene ^{3}**1N**	25.3
azirine **2A**	0.0
azirine **2B**	6.8

could be formed via a concerted reaction of the singlet excited state (S_1) of **1** or through the formation of singlet nitrene ^{1}**1N**. Theoretically, S_1 of **1** could also intersystem cross to its triplet excited state (T_1), extrude a nitrogen atom to form ^{3}**1N**, and finally yield azirine **2** (Scheme 2). Generally, triplet phenylnitrene derivatives dimerize to form the corresponding azo dimers. Larger triplet arylnitrenes, such as 1- and 2-pyrenylnitrenes and 1- and 2-naphthalenylnitrenes, also form azo dimers.[5b,20] Thus, the product studies did not clarify whether the reactivity of **1** occurs on its singlet or triplet surface.

ESR Studies at 80 K. To identify whether photoproducts **5** and **5′** are formed from ^{3}**1N**, we used ESR spectroscopy to detect this intermediate directly. A glassy matrix of **1** in argon-saturated methyl tetrahydrofuran (mTHF) at 80 K was irradiated with a mercury arc lamp, and the ESR spectrum was recorded between 0 and 10,000 G. Figure 1 shows the evolution of the ESR signal as a function of irradiation time. ESR signal characteristics were observed at 6124 and 6199 G, which correspond to the characteristic X_2 and Y_2 lines of a triplet arylnitrene. In addition, a broad signal was observed at ~4500 G for the Z_1 transition. Owing to the broadness of this signal, the exact position of the Z_1 line was uncertain; thus, it was not used to calculate the zero-field splitting (ZFS) parameters *D* and *E*. Instead, the ZFS parameters (D/hc = 0.7442 cm^{-1} and E/hc = 0.00165 cm^{-1}) were calculated by solving Wasserman's equations with the values obtained for the X_2 and Y_2 lines.[21] The low D/hc value indicates significant delocalization of the unpaired electrons in ^{3}**1N**.

The ESR splitting parameters of ^{3}**1N** are expected to be similar to those of other arylnitrenes. The obtained D/hc value corresponds well to those of aromatic nitrenes such as triplet 1-pyrenylnitrene (0.7300)[22] and 1-naphthylnitrene (0.7930)[23] but is smaller than those of phenylnitrene (0.9978)[24] and 2-naphthylnitrene (0.9250) (Scheme 3).[23,25] Wentrup and co-workers have demonstrated a linear correlation between the calculated spin densities of triplet nitrene derivatives and their D/hc values, and ^{3}**1N** followed the same trend.[25] The calculated spin density on the N atom of ^{3}**1N** was 1.44, comparable to those of 1-naphthylnitrene and 1-pyrenylnitrene, which have the most similar D/hc values. However, the spin-density calculations revealed that ^{3}**1N** has more 1,3-biradical character, as the adjacent β-C atom had a spin density of 0.51 (Scheme 3). Thus, the unpaired electrons are localized on the C═C−N moiety and the spin density of ^{3}**1N** is similar to those of triplet vinylnitrenes ^{3}**10**−^{3e}**13** (Scheme 3),[6a,26] although they have greater spin density on the β-C atom.

Low-Temperature Absorption Spectroscopy. Low-temperature absorption spectroscopy provided additional support for the formation of ^{3}**1N**. A glassy matrix of **1** in argon-saturated ethanol, diethyl ether, and isopentane (2:5:5) at 80 K was irradiated at 308 nm, and the absorption was measured periodically. At each time point, the spectrum represents the absorption spectrum of the prephotolyzed matrix subtracted from that of the photolyzed matrix, and Figure 2 shows the changes in the absorption spectra as a function of irradiation time. A new broad absorption band, which appeared between 360 and 450 nm, increased in intensity with irradiation time. In addition, a negative absorption appeared between 310 and 360 nm, which is due to the depletion of **1** and corresponds to its ground state absorption. The new absorption band correlates well with the time-dependent density functional theory (TD-DFT) calculated absorption spectrum of ^{3}**1N** (Figure 2), which has major electronic transitions at 440 (f = 0.0353) and 367 nm (f = 0.0407). In contrast, the TD-DFT-calculated spectra of both the isomers of azirine **2** (Figure S1) did not match the

https://doi.org/10.1021/jacs.4c07846
J. Am. Chem. Soc. XXXX, XXX, XXX−XXX

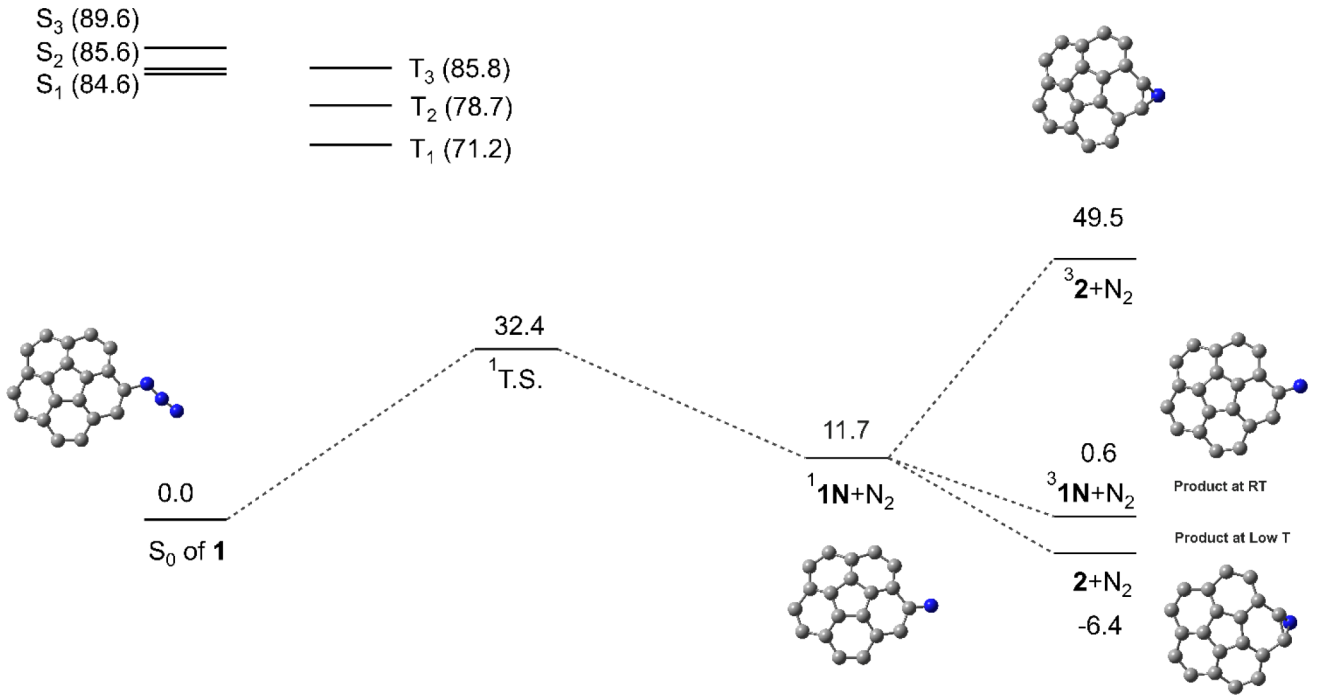

Figure 7. Stationary points on the excited state surface of **1** calculated at the QD-NEVPT2/SA-CASSCF/cc-pVTZ level of theory. Energies are in kcal/mol.

Table 4. Energies of Azirine Conformers 2A and 2B and Their Transition State Calculated at the ωB97-X/def2-TZVP and QD-NEVPT2/CBS Levels of Theory

	E, kcal/mol (ωB97-X/def2-TZVP)	*E*, kcal/mol (QD-NEVPT2)
2A	0	0
TS	34	25.4
2B	1.9	6.8

observed spectrum, thus ruling out azirine **2** as the major product at 80 K.

To correlate the reactivity at 80 K with the product studies at ambient temperature, after irradiating **1** in mTHF at 80 K, the matrix was warmed to ambient temperature and the absorption spectrum was recorded (Figure S2−S9). HRMS analysis of the irradiated solution confirmed the formation of azirine **2**. Furthermore, after adding ethanol and HCl to the solution, HRMS analysis confirmed the formation of the ethanol derivatives of **5** and **5'**.

Laser Flash Photolysis. After verifying that irradiation of **1** in cryogenic matrices produces triplet nitrene ^{3}**1N**, we used laser flash photolysis of **1** to demonstrate that ^{3}**1N** is also formed at ambient temperature. Laser excitation (308 or 266 nm) of **1** in argon-saturated acetonitrile resulted in a broad transient between 330 and 460 nm with λ_{max} at ∼400 nm (Figure 3A). We assigned this transient to ^{3}**1N** by comparison with the absorption spectrum obtained by irradiating **1** in a glassy matrix at 80 K (Figure 2). It should be noted that the TD-DFT-calculated spectra of T_1 of **1** does not fit as well with the observed spectrum (Figure S10).

Analysis of the kinetics revealed that ^{3}**1N** has a lifetime on the order of nanoseconds and is formed faster than the time resolution of the laser (2−3 ns). In the presence of argon, the transient decays with a rate constant of 3.73×10^6 s^{-1} (τ = 268 ns), whereas in in the presence of oxygen, the decay rate constant is 5.95×10^6 s^{-1} (τ = 168 ns). Based on the estimated oxygen concentrations in air- and oxygen-saturated acetonitrile (0.0019 and 0.0091 M),[27] the rate constant for quenching the transient absorption is between 6.5×10^8 and 2.0×10^9 M^{-1} s^{-1}.

Thus, laser flash photolysis demonstrates that the physical properties of ^{3}**1N** differ from those of triplet phenyl- and arylnitrene derivatives, such as 1- and 2-pyrene and 1- and 2-naphthalene nitrenes, which are long-lived with lifetimes on the order of milliseconds and decay by dimerization. In contrast, the nanosecond lifetime of ^{3}**1N** is similar to those of triplet vinylnitrene intermediates. In addition, the rate constant for the reaction of oxygen with ^{3}**1N** is much larger than that for phenyl- and alkylnitrenes[5a,8(a),28] but similar to that for vinylnitrenes (typically $7-20 \times 10^8$ M^{-1} s^{-1}).[29] Because it has a lifetime of a few nanoseconds in argon-saturated acetonitrile, is efficiently quenched by oxygen owing to the significant spin density on the β-C atom, and it decays to form an azirine through intersystem crossing, we propose that ^{3}**1N** is better described as a localized triplet vinylnitrene.[26b]

Calculations. We used calculations to provide insights into why ^{3}**1N** behaves like a triplet vinylnitrene rather than a triplet arylnitrene. The structures of **1**, T_1 of **1**, ^{3}**1N**, and **2** were optimized using DFT calculations at the B3LYP/6-311++G(d,p) level of theory and plotted stationary points on the triplet reaction surface. Two different conformers of **1** (A and B) were optimized. Conformer A, with the azido group facing away from the aromatic ring to which it is connected, is 2 kcal/mol more stable than conformer B, with the azido group directed toward the aromatic ring (Figure 4). Optimization of **1A** and **1B** as a triplet yielded T_1 of **1A** and T_1 of **1B** located 54.6 and 53.2 kcal/mol above S_0 of **1A**, respectively. Spin-density calculations for T_1 of **1A** showed that the unpaired electrons are mainly located on the aromatic ring, with only a small contribution on the azido chromophore (Figure 5). Despite multiple attempts, no transition state connecting T_1 of

https://doi.org/10.1021/jacs.4c07846
J. Am. Chem. Soc. XXXX, XXX, XXX−XXX

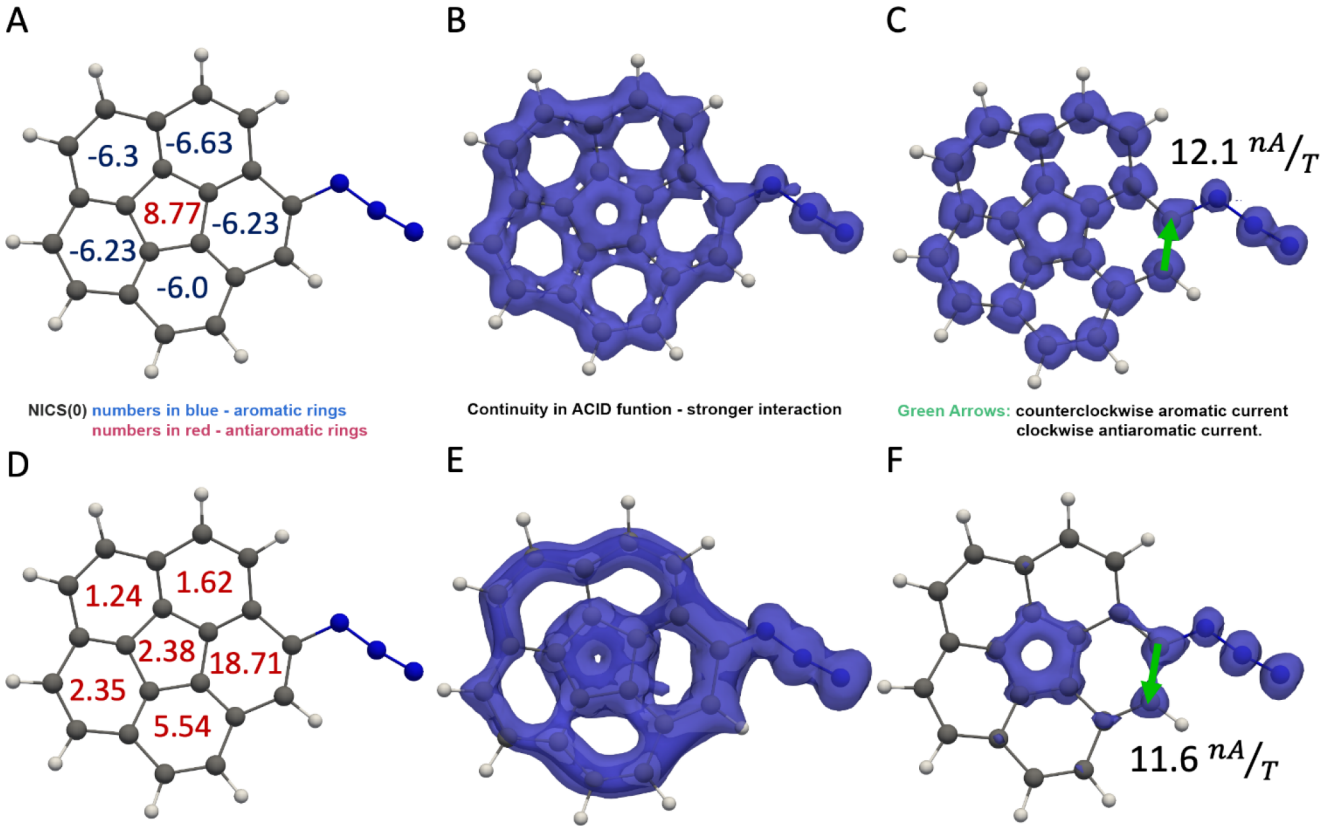

Figure 8. (A) NICS(0) indices calculated using the gauge-invariant atomic orbital (GIAO) method for S_0 of **1**. ACID isosurfaces of S_0 of **1** at cutoff values of (B) 0.003 and (C) 0.005. (D) NICS(0) indices calculated using the GIAO method for T_1 of **1**. ACID isosurfaces of T_1 of **1A** at cutoff values of (E) 0.0003 and (F) 0.003. Green arrows indicate the integrated ring current direction.

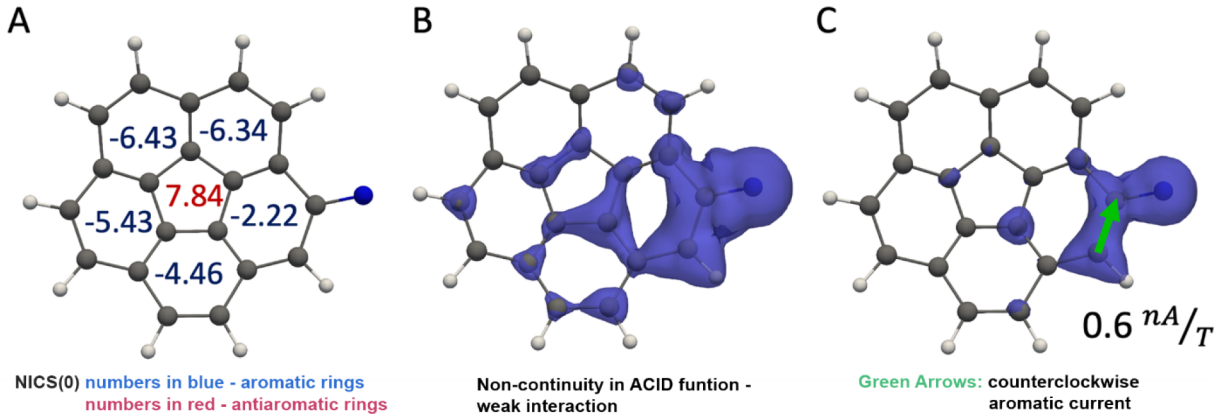

Figure 9. (A) NICS(0) indices calculated using the GIAO method for ^{3}**1N**, ACID isosurfaces of ^{3}**1N** at cutoff values of (B) 0.0001 and (C) 0.0005. The green arrow indicates the integrated ring current direction.

1 to triplet nitrene ^{3}**1N** could be found, presumably, because T_1 of **1** is located on the aromatic part of the molecule and not the azido moiety.

Spin-density calculations for the optimized structure of ^{3}**1N** showed that the unpaired electrons are mainly located on the N atom (1.4) and β-C atom (0.5) (Figure 5). Owing to the dynamic nature of the corannulene ring, ^{3}**1N** can undergo ring inversion. The transition state associated with this process is completely flat and is 9 kcal/mol above ^{3}**1N**. Therefore, direct comparison of the spin densities for this transition state structure and curved ^{3}**1N** can provide important insights into the effect of curvature on spin densities. As shown in Figure 5, curvature does not change the spin densities. Finally, we used the broken symmetry method to optimize the singlet configuration of ^{1}**1N**, which was located 13.5 kcal/mol above ^{3}**1N**. It should be noted that the broken symmetry method yielded total spin $\langle S^2 \rangle$ values of 0.9592 suggesting a significant spin contamination from the triplet state, and therefore this method is not accurate in estimating the energy between singlet and triplet nitrenes.[10b]

Comparison of the calculated bowl depth for **1** (0.093 Å), T_1 of **1** (0.105 Å), ^{3}**1N** (0.091 Å), and **2A** (0.093 Å) showed that T_1 of **1** has a deeper bowl than S_0 of **1**, whereas ^{3}**1N** has the shallowest bowl. The depth of corannulene itself was determined to be 0.086 Å from its crystal structure.[30] Presumably, ^{3}**1N** is the least curved because the unpaired

https://doi.org/10.1021/jacs.4c07846
J. Am. Chem. Soc. XXXX, XXX, XXX−XXX

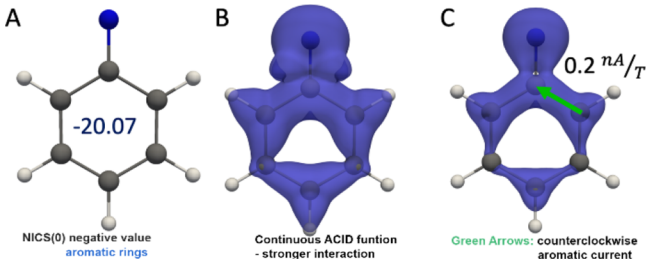

Figure 10. (A) NICS(0) indices calculated using the GIAO method for triplet phenylnitrene. ACID isosurfaces of the triplet phenylnitrene at cutoff values of (B) 0.0001 and (C) 0.0005. The green arrow indicates the integrated ring current direction.

electrons are localized on the vinyl bond. Consequently, the C−C bond has significant single bond character (1.46 Å), which releases some of the strain associated with the curved π-surface. Similar results have been observed for corannulene derivatives, in which cleavage of an outer rim C−C bond causes the bowl to flatten.[31]

We optimized the two possible isomers of azirine **2** (**2A** and **2B**, which have the azirine moiety on the convex and concave sides, respectively, relative to the corannulene bowl), and found that **2B** was 2 kcal/mol less stable than **2A**. We also optimized the triplet configurations of **2** (^{3}**2A** and ^{3}**2B**), which were located 58 and 57 kcal/mol above ^{3}**1N**, respectively. As the energy gap is too large for ^{3}**1N** to form ^{3}**2**, we can rule out azirine **2** being formed by ^{3}**1N** rearranging into ^{3}**2** followed by intersystem crossing. Interestingly, the energy gap between the singlet nitrene ^{1}**1N** and azirine **2** is small (only 2.3 kcal/mol). The calculated stationary points on the surface of **1** for the formation of nitrenes ^{1}**1N** and ^{3}**1N** and azirine **2** are plotted in Figure 6.

To better estimate the energy gap between the singlet and triplet configurations of **1N**, we optimized ^{1}**1N** using the broken symmetry method at the ωB97-X/def2-TZVP level of theory. The calculated energy difference between the singlet and triplet configurations of **1N** (~7.2 kcal/mol) is not significantly different from the calculated singlet−triplet energy gaps for pyrene nitrenes (6.2 kcal/mol for α-pyrene nitrene and 9.5 kcal/mol for β-pyrene nitrene; Table 1). The calculated energy gap between the singlet and triplet configurations of **1N** is also smaller than that measured for triplet phenylnitrene (14.9 kcal/mol)[32] and similar to those reported for triplet oxycarbonyl nitrenes, which undergo intersystem crossing in solution at ambient temperature.[33] Therefore, ^{3}**1N** is likely formed by the intersystem crossing of ^{1}**1N** in solution.

Nitrene ^{3}**1N** exhibits unimolecular reactivity, whereas triplet phenyl, 1- and 2-naphthalene, and 1- and 2-pyrene nitrenes dimerize, despite the localization of their unpaired electrons being similar (Scheme 3). To understand the origin of this difference, we compared the calculated energies of these arylnitrenes to those of the corresponding azirine products using a higher level of theory (ωB97-X/def2-TZVP; Table 2).[34,35] These calculations demonstrate that nitrene ^{3}**1N** and azirine **2** have similar stabilities. In contrast, as the naphthalene and pyrene nitrenes are more stable than their corresponding azirines, they decay by dimerization instead of intersystem crossing to form azirines.

We also used a higher level of theory to clarify the energy gap between nitrene ^{3}**1N** and **2**. At the ωB97-X/def2-TZVP level of theory, the ΔE value becomes minuscular (0.3 kcal/mol). Therefore, we determined ΔE using a multireference method, which is more appropriate because of the expected quasidegeneracy of the singlet and triplet electronic states. CASSCF was implemented in ORCA 5.0.3[36] with averaging over nine triplet and six singlet electronic states, including the ground state.[37] We found that a relatively small active space ($10e^-/10o$) and this state-averaging scheme sufficiently represented the major excitations. The results are summarized in Table 3.

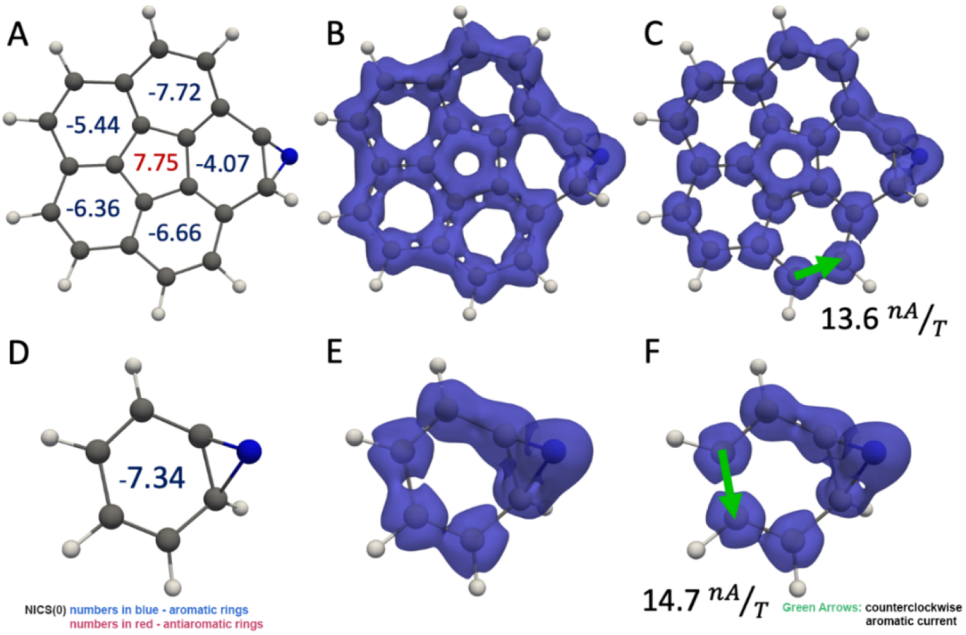

Figure 11. (A) NICS(0) indices calculated using the GIAO method for S_0 of **2A**. ACID isosurfaces of S_0 of **2A** at cutoff values of (B) 0.003 and (C) 0.005. (D) NICS(0) indices calculated using the GIAO method for the ground state of phenyl azirine and ACID isosurfaces of the S_0 state of phenyl azirine at cutoff values of (E) 0.003 and (F) 0.005. Green arrows indicate the integrated ring current direction.

https://doi.org/10.1021/jacs.4c07846
J. Am. Chem. Soc. XXXX, XXX, XXX−XXX

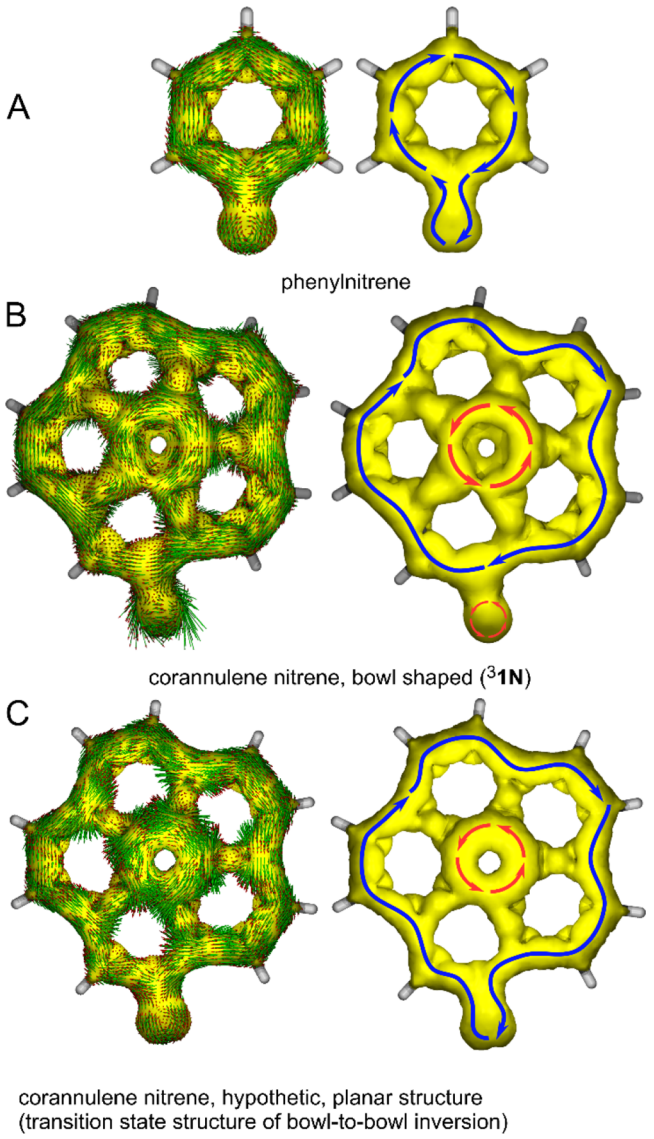

Figure 12. ACID plot of phenylnitrene (A), corannulene nitrene ^{3}**1N** (B) and planarized corannulene nitrene (C). For clarity, the ring currents are additionally represented schematically to the right of each ACID plot (diatropic currents in blue, paratropic currents in red). The structures were optimized at the B3LYP/6-311++G(d,p)[42] level of density functional theory. The ACID plot is calculated from the current density tensor field using the AICD program.[43] The current densities were calculated using the CSGT method[44] (Gaussian 16 Rev. A.03 keywords: NMR = CSGT, iop(10/93 = 2)[45] based on a B3LYP/6-311++G(d,p) wave function. Only π orbitals (orbitals with A2 and B1 symmetry, C2v point group) are included in the ACID plot. The isosurface value for the ACID plot is 0.03. Current density vectors are plotted on top of the ACID surface. The lengths of the vectors are proportional to the absolute values of the current densities. The magnetic field is oriented orthogonally to the ring plane and points toward the viewer. CIV values are available in the SI.

According to this data, **2A** and **2B** are lower in energy than ^{3}**1N**, and **2A** is the more stable isomer of azirine **2**. As nitrene ^{3}**1N** undergoes intersystem crossing to the singlet surface, it reaches the lowest energy structure, which is **2A**. As the rate of this process is only limited by the intersystem crossing rate constant, it competes with other reactions on the triplet surface, thus preventing ^{3}**1N** from dimerizing.

According to DFT calculations at the ωB97-X/def2-TZVP level of theory, the corannulene azirine has two conformers, in which the azirine ring is bent into or out of the corannulene moiety (Figure 7). To estimate the energy barrier between these conformers, we located and optimized the transition state (Figure 7) using the nudged elastic band method in ORCA 5.0.3 at the ωB97-X/def2-TZVP level of theory.[38] The transition state closely resembles ^{3}**1N**. The energy values are summarized in Table 4. According to this data, the energy barrier is slightly overestimated at the ωB97-X/def2-TZVP level of theory. With an energy barrier as low as 25.4 kcal/mol, thermal conversion between the two conformers is possible, which makes it possible for both isomers to contribute to products formation.

To obtain energy diagram for the triplet reactivity of **1**, we optimized structures of **1A**, ^{1}**1N**, ^{3}**1N**, **2B**, and ^{3}**2B** at the B3LYP-D4/ma-def2-TZVP level of theory, calculated their single-point energies using QD-NEVPT2/SA-CASSCF/cc-pVTZ level of theory and plotted the stationary points on the triplet reaction surface of **1** for the formation of nitrenes ^{1}**1N**, ^{3}**1N**, and azirine **2** (Figure 7). The vertical energies of the first, second, and third singlet excited states of **1**, were located 84.6, 85.6, and 89.1 kcal/mol, respectively, above the ground state (S_0). Similarly, we located T_1, T_2, and T_3 at 71.2, 78.7, and 85.8 kcal/mol, respectively, above S_0 of **1**. Nitrene ^{1}**1N** was located 11.1 kcal/mol above its triplet configuration. Azirine **2B** was 5.8 kcal/mol more stable than ^{3}**1N**. Details of these calculations are provided in the section of CASSCF calculations.

Finally, the aromaticities of **1**, T_1 of **1**, ^{3}**1N**, and **2** were investigated to address why nitrene ^{3}**1N** is best described as a localized vinylnitrene rather than an aromatic nitrene. Owing to their polycyclic nature, the aromaticity of these compounds cannot be assessed by simply applying Hückel's and Baird's rules. Instead, the aromaticity was evaluated using calculation methods to estimate the π-electron current and resulting induced magnetic field.[39]

We used nucleus-independent chemical shift (NICS) calculations[40] to characterize the aromatic properties. In this analysis, negative and positive values correspond to aromatic and antiaromatic rings, respectively, and the absolute value is related to the induced current magnitude. The aromatic properties were also estimated from the π-electron currents obtained using anisotropy of the induced current density (ACID) calculations. Although the ACID method does not allow explicit determination of aromaticity or antiaromaticity, the localization of magnetically induced current densities can be analyzed and plotted as an isosurface at different cutoff values. By visually investigating the ACID function shape and comparing its continuity with those of other species more pronounced aromaticity or antiaromaticity can be pointed out. In addition, the magnetically induced ring currents through selected chemical bonds are intended to aid in the characterization.

The magnetic properties of **1** (Figure 8A–C) are similar to those reported for corannulene itself.[41] NICS(0) indexing shows that the center ring of **1** has an antiaromatic character, whereas the outer rings are aromatic. The same features are indicated by the ACID function. By varying the isosurface cutoff values to analyze the continuity of the ACID function, it is seen that the center ring demonstrates a more pronounced antiaromaticity. However, this difference is subtle when

https://doi.org/10.1021/jacs.4c07846
J. Am. Chem. Soc. XXXX, XXX, XXX−XXX

comparing the integrated ring currents since they are quite close in magnitude, though opposite in direction.

The NICS(0) analysis indicates that T_1 of **1** is fully antiaromatic (Figure 8D−F), as the NICS(0) values for all the aromatic rings are positive. Notably, the ring with the azido substituent has a significantly larger value (18.71) than the other rings (between 1 and 5). Based on the ACID functions, the rings do not display a continuous electronic current. Instead, it is most evident on the azido-substituted ring. In addition, lower cutoff values were necessary to visualize the function, which indicates it has weaker electronic current compared to **1**. Thus, the ACID function analysis is in good agreement with the NICS(0) calculations, showing that T_1 of **1** is antiaromatic. This strongly antiaromatic nature suggests that T_1 of **1** is highly reactive and short-lived.

The NICS(0) analysis of nitrene ^{3}**1N** reveals an extensive aromatic character (Figure 9), as only the center ring has a positive value. However, in the ACID function analysis, no circular electric currents are present in any of the rings, as highlighted at smaller isosurface cutoff values. These results indicate that the π-conjugation is disrupted in ^{3}**1N** and that the unpaired electrons are localized on the vinyl-N chromophore.

For comparison, we also analyzed triplet phenylnitrene (Figure 10), which displays more pronounced aromatic properties than ^{3}**1N**. The NICS(0) value of triplet phenylnitrene indicates a significant diatropic current. However, the ACID functions are similar to those of ^{3}**1N**, although more continuous at same cutoff values. Therefore, the NICS(0) and ACID data demonstrate that triplet phenylnitrene is aromatic, whereas ^{3}**1N** is a less aromatic species. The integrated ring currents are very weak in both molecules compared to corannulene azide (Figure 8), corannulene azirine and phenyl azirine (Figure 11), which further supports the weak aromaticity of ^{3}**1N**.

The aromatic character of azirine **2A** (Figure 11A−C) is similar to that of S_0 of **1**, as the center ring has a positive NICS(0) value and is antiaromatic, whereas the surrounding rings have negative NICS(0) values and are aromatic. In addition, the azirine-substituted ring has slightly less electronic current than the other rings. According to the ACID function analysis, **1** and **2** exhibit similar π-conjugation, although it is slightly disrupted in the phenyl ring with the azirine substituent owing to its nonplanarity. However, the current distributions of **2A** and ^{3}**1N** differ significantly, as the former exhibits circular currents but the latter does not. The aromaticity of **2A** renders it more stable than the weakly aromatic ^{3}**1N**.

Finally, we calculated the ACID scalar field of the title nitrene ^{3}**1N** and of reference compounds from the current density tensor field using the ACiD program,[43] with the current densities calculated using the CSGT method[44] for both triplet phenylnitrene and ^{3}**1N**. The critical isosurface value (CIV) was calculated for each carbon−carbon bond (Figures S11 and S12) and serves as a measure of the strength of the electronic conjugation between two atoms. To distinguish between aromatic and antiaromatic ring currents, the current density vectors are drawn as arrows (green arrows with red arrow heads) on the isosurface. The vector field of the current density depends on the relative orientation of the molecule to the magnetic field. The convention is to align the magnetic field perpendicular to the ring plane of the molecule under investigation so that the magnetic field vector points toward the observer. Diamagnetic currents then run clockwise and indicate an aromatic system and paramagnetic currents are counterclockwise and indicate antiaromatic systems.

Triplet phenylnitrene, as expected, exhibits a diatropic ring current (clockwise currents in Figure 12A) in the aromatic 6-electron, 6-center π system of the phenyl ring. Remarkably, a considerable part of the ring currents includes the nitrogen atom of the nitrene, indicating an 8-electron, triplet Baird aromatic system.[46]

In agreement with previous calculations[41c] on the parent corannulene, corannulene nitrene (triplet) exhibits a diatropic ring current (clockwise current in Figure 12B) in the aromatic 14-electron periphery and a paratropic ring current (anticlockwise) in the central 5-membered ring. As opposed to phenylnitrene, there is a separate paratropic ring (anticlockwise) current encircling only the nitrogen atom. The nitrogen atom is in conjugation with the aromatic π system, however, a triplet Baird system as in phenylnitrene is not discernible. The strength of aromatic current of ^{3}**1N** is less than for triplet phenylnitrene.

To elucidate the reason for the remarkably different electronic structures of phenylnitrene and corannulene nitrene (^{3}**1N**), we also performed ACID calculations with the hypothetic planar corannulene (transition structure of the bowl-to-bowl inversion, Figure 12C). The ACID analysis shows that the planar corannulene nitrene has topologically very similar ring currents and conjugation with the aromatic ring as phenylnitrene. The nitrogen atom of the nitrene is part of the diatropic ring current in the periphery of the corannulene. The total π system therefore shows Baird aromaticity, as in phenylnitrene. It can be concluded that it is the deformation from the planarity (bowl shape) that changes the electronic structure of corannulene nitrene (^{3}**1N**) and cancels the Baird aromaticity. This is also supported by calculations of coronene nitrene (see SI). Hence, the reactivity of corannulene nitrene should be more similar to that of vinyl nitrene than that of phenylnitrene.

CONCLUSIONS

We investigated the unique reactivity of azidocorannulene **1**. Based on the structures of the products obtained upon photolysis of **1** in the presence of methanol, curvature plays an important role in determining the outcome of the photoreaction. This system is a rare example of corannulene desymmetrization through covalent modification of its carbon network. It should be highlighted that the capturing of azirine **2** with methanol offers a new method for synthesizing substituted dihydrocorannulene derivatives. Spin-density calculations demonstrated that the unpaired electrons in ^{3}**1N** are localized on the vinylnitrene moiety, explaining its efficient quenching by oxygen and consistent with the ZFS parameters obtained using ESR spectroscopy. Furthermore, the calculated spin-densities and ZFS parameters were similar to those of triplet vinylnitrenes, which are well-known to have 1,3-biradical character. As the localization of the unpaired electrons on the vinyl nitrene moiety resulted in the C−C bond having single bond character, the bowl of ^{3}**1N** was less curved than that of **1**. This localization of the unpaired electrons and flattening of the bowl were also reflected in the aromaticity calculations for ^{3}**1N**. Although NICS(0) indexing showed positive values for all the rings, the ACID revealed that the (6-electron) phenyl ring in phenyl nitrene and the 14-electron periphery in corannulene nitrene are aromatic (diatropic ring current). In triplet phenyl nitrene the ring

https://doi.org/10.1021/jacs.4c07846
J. Am. Chem. Soc. XXXX, XXX, XXX−XXX

current partially includes the nitrene, which indicates Baird aromaticity to some extent. This is not the case in corannulene nitrene. Finally, ^{3}**1N** is short-lived because it can decay by intersystem crossing to **2**, which is more stable. The aromaticity of the corannulene rings in **2** stabilizes this species relative to the less aromatic ^{3}**1N**.

■ ASSOCIATED CONTENT

Supporting Information

The Supporting Information is available free of charge at https://pubs.acs.org/doi/10.1021/jacs.4c07846.

Synthesis of **1** product studies, general procedures, IR, NMR, and HRMS spectra of **1** and **5**; Cartesian coordinates, energies, vibrational frequencies of **1**−**5**; ACID plots (PDF)

■ AUTHOR INFORMATION

Corresponding Author

Anna D. Gudmundsdottir − *Department of Chemistry, University of Cincinnati, Cincinnati, Ohio 45221-0172, United States;* orcid.org/0000-0002-5420-4098; Email: anna.gudmundsdottir@uc.edu

Authors

Kelley S. McKissic − *Department of Chemistry, University of Cincinnati, Cincinnati, Ohio 45221-0172, United States*

Mrinal Chakraborty − *Department of Chemistry, University of Cincinnati, Cincinnati, Ohio 45221-0172, United States*

Dmitrii Govorov − *Department of Chemistry, University of Cincinnati, Cincinnati, Ohio 45221-0172, United States*

Mayukh Majumder − *Department of Chemistry and Biochemistry, The Ohio State University, Columbus, Ohio 43210, United States*

DeAnte F. Judkins − *Department of Chemistry, University of Cincinnati, Cincinnati, Ohio 45221-0172, United States*

Rajkumar Merugu − *Department of Chemistry, University of Cincinnati, Cincinnati, Ohio 45221-0172, United States*

H. Dushanee M. Sriyarathne − *Department of Chemistry, University of Cincinnati, Cincinnati, Ohio 45221-0172, United States*

Anushree Das − *Department of Chemistry, University of Cincinnati, Cincinnati, Ohio 45221-0172, United States*

W. Dinindu Mendis − *Department of Chemistry, University of Cincinnati, Cincinnati, Ohio 45221-0172, United States*

Jan-Simon von Glasenapp − *Otto Diels-Institute for Organic Chemistry, University of Kiel, Kiel F-24118, Germany*

Rainer Herges − *Otto Diels-Institute for Organic Chemistry, University of Kiel, Kiel F-24118, Germany;* orcid.org/0000-0002-6396-6991

Christopher M. Hadad − *Department of Chemistry and Biochemistry, The Ohio State University, Columbus, Ohio 43210, United States*

James Mack − *Department of Chemistry, University of Cincinnati, Cincinnati, Ohio 45221-0172, United States;* orcid.org/0000-0001-5717-8916

Manabu Abe − *Department of Chemistry, Hiroshima University, Hiroshima 739-8526, Japan;* orcid.org/0000-0002-2013-4394

Complete contact information is available at: https://pubs.acs.org/10.1021/jacs.4c07846

Author Contributions

[#]K.S.M., M.C., and D.G. contributed equally.

Author Contributions

[§]D.F.J, R.M., H.D.M.S., A.D., and W.D.M. contributed equally.

Notes

The authors declare no competing financial interest.

■ ACKNOWLEDGMENTS

The authors thank the National Science Foundation (CHE-2102248 and CHE-2400227) and the OSC (PES0597) for their generous support. This work used PSC at Bridges-2 RM through allocation CHE240153 from the Advanced Cyberinfrastructure Coordination Ecosystem: Services & Support (ACCESS) program. We thank Dr. Sallans for his help with MS. D.G. and H.D.M.S. are grateful for a Doctoral Enhancement Fellowship from the Department of Chemistry at the University of Cincinnati. R.M. is grateful for a URC Fellowship from the University of Cincinnati. M.A. thanks JSPS KAKENHI (grant nos. JP17H03022, 20K21197, 21H01921, 22K19033) and JST CREST (JPMJCR18R4) for their generous support.

■ REFERENCES

(1) (a) Tsefrikas, V. M.; Scott, L. T. Geodesic Polyarenes by Flash Vacuum Pyrolysis. *Chem. Rev.* **2006**, *106* (12), 4868−4884. From NLM (b) Wu, Y.-T.; Siegel, J. S. Aromatic Molecular-Bowl Hydrocarbons: Synthetic Derivatives, Their Structures, and Physical Properties. *Chemi. Revi.* **2006**, *106* (12), 4843−4867. (c) Barth, W. E.; Lawton, R. G. Dibenzo[*ghi,mno*]Fluoranthene. *J. Am. Chem. Soc.* **1966**, *88* (2), 380−381. (d) Wu, Y. T.; Siegel, J. S. Aromatic Molecular-Bowl Hydrocarbons: Synthetic Derivatives, Their Structures, and Physical Properties. *Chem. Rev.* **2006**, *106* (12), 4843−4867. From NLM

(2) (a) Petrukhina, M. A. From Corannulene to Larger Carbon Bowls: Are They Better for Multiple Metal Encapsulation? *J. Chem. Soc., Dalton Trans.* **2019**, *48* (16), 5125−5130. (b) Zhou, Z.; Petrukhina, M. A. Planar, Curved and Twisted Molecular Nanographenes: Reduction-Induced Alkali Metal Coordination. *Coord. Chem. Rev.* **2023**, *486*, No. 215144.

(3) (a) Leith, G. A.; Shustova, N. B. Graphitic Supramolecular Architectures Based on Corannulene, Fullerene, and Beyond. *Chem. Commun.* **2021**, *57* (79), 10125−10138. (b) Xu, Q.; Petrukhina, M. A.; Rogachev, A. Y. Stepwise Deprotonation of Sumanene: Electronic Structures. *Energetics and Aromaticity Alterations. PhysChemChemPhys.* **2017**, *19* (32), 21575−21583.

(4) ((a)) Muthukrishnan, S.; Ranaweera, R. A. A. U.; Gudmundsdottir, A. D.Triplet Alkyl Nitrene. In *Nitrenes and Nitrenium Ions*; Wiley Series on Reactive Intermediates in Chemistry and Biology, Vol. 6; Falvey, D. E.; Gud-mundsdottir, A. D., Eds.; Wiley, 2013; pp 167−189. (b) Gritsan, N. P.; Platz, M. S. Kinetics, Spectroscopy, and Computational Chemistry of Arylnitrenes. *Chemi. Revi.* **2006**, *106* (9), 3844−3867. (c) Wentrup, C. Carbenes and Nitrenes: Recent Developments in Fundamental Chemistry. *Angew. Chem. Int.Ed.* **2018**, *57* (36), 11508−11521. (d) Wentrup, C. Nitrenes, Carbenes, Diradicals, and Ylides. Interconversions of Reactive Intermediates. *Acc. Chem. Res.* **2011**, *44* (6), 393−404.

(5) (a) Singh, P. N. D.; Mandel, S. M.; Sankaranarayanan, J.; Muthukrishnan, S.; Chang, M.; Robinson, R. M.; Lahti, P. M.; Ault, B. S.; Gudmundsdóttir, A. D. Selective Formation of Triplet Alkyl Nitrenes from Photolysis of $\hat{I}^2$-Azido-Propiophenone and Their Reactivity. *J. Am. Chem. Soc.* **2007**, *129* (51), 16263−16272. (b) Schrock, A. K.; Schuster, G. B. Photochemistry of Naphthyl and Pyrenyl Azides: Chemical Properties of the Transient Intermediates Probed by Laser Spectroscopy. *J. Am. Chem. Soc.* **1984**, *106* (18), 5234−5240.

(6) (a) Sarkar, S. K.; Sawai, A.; Kanahara, K.; Wentrup, C.; Abe, M.; Gudmundsdottir, A. D. Direct Detection of a Triplet Vinylnitrene, 1,4-Naphthoquinone-2-Ylnitrene, in Solution and Cryogenic Matrices. *J. Am. Chem. Soc.* **2015**, *137* (12), 4207−4214. (b) Qian, W.; Schreiner, P. R.; Mardyukov, A. Preparation and Photochemistry of Parent Triplet Vinylarsinidene. *J. Am. Chem. Soc.* **2024**, *146* (1), 930−935.

(7) (a) Ahmed, N.; Kavikarage, J. P. K.; Judkins, D. F.; Mendis, W. D.; Merugu, R.; Krause, J. A.; Ault, B. S.; Gudmundsdottir, A. D. Unraveling the Solid-State Photoreactivity of Carbonylbis(4,1-phenylene)dicarbonazidate with Laser Flash Photolysis. *J. Phys. Chem. A* **2023**, *127* (46), 9705−9716. (b) Sigman, M. E.; Autrey, T.; Schuster, G. B. Aroylnitrenes with Singlet Ground States: Photochemistry of Acetyl-Substituted Aroyl and Aryloxycarbonyl Azides. *J. Am. Chem. Soc.* **1988**, *110* (13), 4297−4305.

(8) ((a)) Schuster, G. B.; Platz, M. S.Photochemistry of Phenyl Azide. In *Adv. Photochem.*, Vol. *17*; Volman, D. H.; Hammond, G. S; Neckers, D. C., Eds.; John Wiley & Sons, Inc., 1992; pp 69−143. DOI: . ((b)) Platz, M. S.Nitrene. In *Reactive Intermediate Chemistry*; Moss, R. A.; Platz, M. S.; Jones, M. J., Eds.; Wiley, 2004; pp 501−559.

(9) (a) Hershfield, R.; Bender, M. L. Nucleophilic and Metal Ion Acceleration of Ester Hydrolysis in a Hydrophobic Complex. Reactive Enzyme Model System. *J. Am. Chem. Soc.* **1972**, *94* (4), 1376−1377. (b) Tsao, M.-L.; Platz, M. S. Photochemistry of Ortho, Ortho' Dialkyl Phenyl Azides. *J. Am. Chem. Soc.* **2003**, *125* (39), 12014−12025. (c) Gritsan, N. P.; Zhai, H. B.; Yuzawa, T.; Karweik, D.; Brooke, J.; Platz, M. S. Spectroscopy and Kinetics of Singlet Perfluoro-4-Biphenylnitrene and Singlet Perfluorophenylnitrene. *J. Phys. Chem. A* **1997**, *101* (15), 2833−2840.

(10) (a) Mitchell, J. K.; Hussain, W. A.; Bansode, A. H.; O'Connor, R. M.; Parasram, M. Aziridination Via Nitrogen-Atom Transfer to Olefins from Photoexcited Azoxy-Triazenes. *J. Am. Chem. Soc.* **2024**, *146* (14), 9499−9505. (b) George, S.; Govorov, D.; Gatlin, D. M.; Merugu, R.; Wasson, F. J.; Shields, D. J.; Allen, Y.; Muthukrishnan, S.; Krause, J. A.; Abe, M.; Gudmundsdottir, A. D. Light-Mediated Synthesis of 2-(4-Methoxyphenyl)-1-pyrroline via Intramolecular Reductive Cyclization of a Triplet Alkylnitrene. *Org. Lett.* **2023**, *25* (23), 4345−4349. (c) Bouayad-Gervais, S.; Nielsen, C. D. T.; Turksoy, A.; Sperger, T.; Deckers, K.; Schoenebeck, F. Access to Cyclic N-Trifluoromethyl Ureas through Photocatalytic Activation of Carbamoyl Azides. *J. Am. Chem. Soc.* **2022**, *144* (13), 6100−6106. (d) Scholz, S. O.; Farney, E. P.; Kim, S.; Bates, D. M.; Yoon, T. P. Spin-Selective Generation of Triplet Nitrenes: Olefin Aziridination through Visible-Light Photosensitization of Azidoformates. *Angew. Chem. Int.Ed.* **2016**, *55* (6), 2239−2242. (e) Farney, E. P.; Yoon, T. P. Visible-Light Sensitization of Vinyl Azides by Transition-Metal Photocatalysis. *Angew. Chem. Int.Ed.* **2014**, *53* (3), 793−797. (f) Donnelly, K.; Baumann, M. Continuous Flow Technology as an Enabler for Innovative Transformations Exploiting Carbenes, Nitrenes, and Benzynes. *J. Org. Chem.* **2022**, *87* (13), 8279−8288. ((g)) Lee, K.; Seo, K.; Dehghany, M.; Hu, Y.; Trinh, A.; Schomaker, J. M.An Overview of N-Heterocycle Syntheses Involving Nitrene Transfer Reactions. In *Heterocycles from Carbenes and Nitrenes: Methods, Reactions and Synthetic Applications*, Topics in Heterocyclic Chemistry, Vol. *59*; Doyle, M. P.; Xu, X., Eds.; Springer International Publishing, 2023; pp 313−377. DOI: . (h) Ye, C.-X.; Meggers, E. Chiral-at-Ruthenium Catalysts for Nitrene-Mediated Asymmetric C−H Functionalizations. *Acc. Chem. Res.* **2023**, *56* (9), 1128−1141. (i) van Vliet, K. M.; de Bruin, B. Dioxazolones: Stable Substrates for the Catalytic Transfer of Acyl Nitrenes. *ACS Catal.* **2020**, *10* (8), 4751−4769. (j) Zhu, J. S.; Li, C. J.; Tsui, K. Y.; Kraemer, N.; Son, J.-H.; Haddadin, M. J.; Tantillo, D. J.; Kurth, M. J. Accessing Multiple Classes of *2H*-Indazoles: Mechanistic Implications for the Cadogan and Davis−Beirut Reactions. *J. Am. Chem. Soc.* **2019**, *141* (15), 6247−6253.

(11) (a) Schmidt-Räntsch, T.; Verplancke, H.; Lienert, J. N.; Demeshko, S.; Otte, M.; Van Trieste, G. P., III; Reid, K. A.; Reibenspies, J. H.; Powers, D. C.; Holthausen, M. C.; Schneider, S. Nitrogen Atom Transfer Catalysis by Metallonitrene C−H Insertion: Photocatalytic Amidation of Aldehydes. *Angew. Chem., Int. Ed.* **2022**, *61* (9), No. e202115626. (b) Sun, J.; Abbenseth, J.; Verplancke, H.; Diefenbach, M.; de Bruin, B.; Hunger, D.; Würtele, C.; van Slageren, J.; Holthausen, M. C.; Schneider, S. A Platinum(II) Metallonitrene with a Triplet Ground State. *Nat. Chem.* **2020**, *12* (11), 1054−1059. (c) Thornton, A. R.; Martin, V. I.; Blakey, S. B. π-Nucleophile Traps for Metallonitrene/Alkyne Cascade Reactions: A Versatile Process for the Synthesis of α-Aminocyclopropanes and β-Aminostyrenes. *J. Am. Chem. Soc.* **2009**, *131* (7), 2434−2435.

(12) (a) Kuwashima, S.-Y.; Kubota, M.; Kushida, K.; Ishida, T.; Ohashi, M.; Nogami, T. Synthesis and Structure of Nitrene-C_{60} Adduct C_{60}Nphth (Phth = Phthalimido). *Tetrahedron Lett.* **1994**, *35* (25), 4371−4374. (b) Akhmetov, A. R.; Tuktarov, A. R.; Popod'ko, N. y. R.; Dzhemilev, U. M. Cycloaddition of Alkyl Azides to Fullerene C60 in the Presence of $Cu(OTf)_2$. *Mendeleev Commun.* **2015**, *25* (5), 346−347.

(13) (a) Rigaudy, J.; Igier, C.; Barcelo, J. Directing Effect of Bases on the Photo-Reactions of Polycyclic Aromatic Azides. Synthesis of "Ortho-Fused" Azepines in the Anthracene and Naphthalene Series. *Tetrahedron Lett.* **1975**, *16* (44), 3845−3848. (b) Tsao, M.-L.; Platz, M. S. Flash Photolysis of the Naphthyl Azides with Uv−Vis and Ir Detection of Intermediates. *J. Phys. Chem. A* **2004**, *108* (7), 1169−1176. (c) Wang, J.; Burdzinski, G.; Zhu, Z.; Platz, M. S.; Carra, C.; Bally, T. Ultrafast Spectroscopic and Matrix Isolation Studies of P-Biphenylyl, O-Biphenylyl, and 1-Naphthylnitrenium Cations. *J. Am. Chem. Soc.* **2007**, *129* (26), 8380−8388.

(14) Sygula, A.; Sygula, R.; Fronczek, F. R.; Rabideau, P. W. Addition of Organolithium Reagents to Corannulene and Conformational Preferences in 1-Alkyl-1,2-Dihydrocorannulenes. *J. Org. Chem.* **2002**, *67* (18), 6487−6492.

(15) Nakajima, K.; Ashida, Y.; Nojima, S.; Nishibayashi, Y. Radical Addition to Corannulene Mediated by Visible-Light-Photoredox Catalysts. *Chem. Lett.* **2015**, *44* (4), 545−547.

(16) Carroll, S. E.; Nay, B.; Scriven, E. F. V.; Suschitzky, H.; Thomas, D. R. Decomposition of Aromatic Azides in Ethanethiol. *Tetrahedron Lett.* **1977**, *18* (36), 3175−3178.

(17) Leyva, E.; Platz, M. S. The Temperature Dependent Photochemistry of 1-Naphthyl Azide. *Tetrahedron Lett.* **1987**, *28* (1), 11−14.

(18) Nay, B.; Scriven, E. F. V.; Suschitzky, H.; Khan, Z. U. Photolysis of Naphthyl and Quinolyl Azides; Part Ii. Synthesis of Bicyclic Azepines and Quinolyl O-Diamines. *Synthesis* **1977**, *1977* (11), 757−758.

(19) (a) Seiders, T. J.; Baldridge, K. K.; Elliott, E. L.; Grube, G. H.; Siegel, J. S. Synthesis and Quantum Mechanical Structure of Sym-Pentamethylcorannulene and Decamethylcorannulene. *J. Am. Chem. Soc.* **1999**, *121* (32), 7439−7440. (b) Biedermann, P. U.; Pogodin, S.; Agranat, I. Inversion Barrier of Corannulene. A Benchmark for Bowl-to-Bowl Inversions in Fullerene Fragments. *J. Org. Chem.* **1999**, *64* (10), 3655−3662. (c) Seiders, T. J.; Baldridge, K. K.; Grube, G. H.; Siegel, J. S. Structure/Energy Correlation of Bowl Depth and Inversion Barrier in Corannulene Derivatives: Combined Experimental and Quantum Mechanical Analysis. *J. Am. Chem. Soc.* **2001**, *123* (4), 517−525. (d) Scott, L. T.; Hashemi, M. M.; Bratcher, M. S. Corannulene Bowl-to-Bowl Inversion Is Rapid at Room Temperature. *J. Am. Chem. Soc.* **1992**, *114* (5), 1920−1921.

(20) (a) Tsuguo, Y.; Hiroshi, K.; Saburo, N. The Photo-Decomposition of 1-Azidopyrene in the Benzene Solution. *Bull. Chem. Soc. Jpn.* **1972**, *45* (2), 361−365. (b) Wang, J.; Kubicki, J.; Burdzinski, G.; Hackett, J. C.; Gustafson, T. L.; Hadad, C. M.; Platz, M. S. Early Events in the Photochemistry of 2-Naphthyl Azide from Femtosecond Uv/Vis Spectroscopy and Quantum Chemical Calculations: Direct Observation of a Very Short-Lived Singlet Nitrene. *J. Org. Chem.* **2007**, *72* (20), 7581−7586.

(21) Wasserman, E.; Snyder, L. C.; Yager, W. A. Esr of the Triplet States of Randomly Oriented Molecules. *J. Chem. Phys.* **1964**, *41* (6), 1763−1772.

https://doi.org/10.1021/jacs.4c07846
J. Am. Chem. Soc. XXXX, XXX, XXX−XXX

(22) Yamaoka, T.; Kashiwagi, H.; Nagakura, S. The Photo-Decomposition of 1-Azidopyrene in the Benzene Solution. *Bull. Chem. Soc. Jpn.* **1972**, *45* (2), 361−365.
(23) Kuzaj, M.; Lüerssen, H.; Wentrup, C. Esr Observation of Thermally Produced Triplet Nitrenes and Photochemically Produced Triplet Cycloheptatrienylidenes. *Angew. Chem., Int. Ed.* **1986**, *25* (5), 480−482.
(24) Wasserman, E. Electron Spin Resonance of Nitrenes. *Prog. Phys. Org. Chem.* **1971**, *8*, 319−336.
(25) Kvaskoff, D.; Bednarek, P.; George, L.; Waich, K.; Wentrup, C. Nitrenes, Diradicals, and Ylides. Ring Expansion and Ring Opening in 2-Quinazolylnitrenes. *J. Org. Chem.* **2006**, *71* (11), 4049−4058.
(26) (a) Shields, D. J.; Sarkar, S. K.; Sriyarathne, H. D. M.; Brown, J. R.; Wentrup, C.; Abe, M.; Gudmundsdottir, A. D. Transforming Triplet Vinylnitrene into Triplet Alkylnitrene at Cryogenic Temperatures. *Org. Lett.* **2019**, *21* (18), 7194−7198. (b) Sarkar, S. K.; Osisioma, O.; Karney, W. L.; Abe, M.; Gudmundsdottir, A. D. Using Molecular Architecture to Control the Reactivity of a Triplet Vinylnitrene. *J. Am. Chem. Soc.* **2016**, *138* (45), 14905−14914. (c) Gatlin, D. M.; Karney, W. L.; Abe, M.; Ault, B. S.; Gudmundsdottir, A. D. Formation and Reactivity of Triplet Vinylnitrenes as a Function of Ring Size. *J. Org. Chem.* **2019**, *84* (14), 9215−9225.
(27) Battino, R. *Solubility Data Series: Vol. 7, Oxygen and Ozone*; Pergamon, Oxford, Englan, 1981.
(28) Liang, T. Y.; Schuster, G. B. Photochemistry of 3- and 4-Nitrophenyl Azide: Detection and Characterization of Reactive Intermediates. *J. Am. Chem. Soc.* **1987**, *109* (25), 7803−7810.
(29) Zhang, X.; Sarkar, S. K.; Weragoda, G. K.; Rajam, S.; Ault, B. S.; Gudmundsdottir, A. D. Comparison of the Photochemistry of 3-Methyl-2-phenyl-2*H*-azirine and 2-Methyl-3-phenyl-2*H*-azirine. *J. Org. Chem.* **2014**, *79* (2), 653−663.
(30) Hanson, J. C.; Nordman, C. E. The Crystal and Molecular Structure of Corannulene, $C_{20}H_{10}$. *Acta Crystallogr. B* **1976**, *32* (4), 1147−1153.
(31) (a) Wu, Y.-F.; Ying, S.-W.; Su, L.-Y.; Du, J.-J.; Zhang, L.; Chen, B.-W.; Tian, H.-R.; Xu, H.; Zhang, M.-L.; Yan, X.; et al. Nitrogen-Embedded Quintuple [7]Helicene: A Helicene−Azacorannulene Hybrid with Strong near-Infrared Fluorescence. *J. Am. Chem. Soc.* **2022**, *144* (24), 10736−10742. (b) Leith, G. A.; Rice, A. M.; Yarbrough, B. J.; Kittikhunnatham, P.; Mathur, A.; Morris, N. A.; Francis, M. J.; Berseneva, A. A.; Dhull, P.; Adams, R. D.; et al. Broken-Hearted" Carbon Bowl Via Electron Shuttle Reaction: Energetics and Electron Coupling. *Chem. Sci.* **2021**, *12* (19), 6600−6606. (c) Yokoi, H.; Hiroto, S.; Shinokubo, H. Reversible σ-Bond Formation in Bowl-Shaped π-Radical Cations: The Effects of Curved and Planar Structures. *J. Am. Chem. Soc.* **2018**, *140* (13), 4649−4655.
(32) (a) Travers, M. J.; Cowles, D. C.; Clifford, E. P.; Ellison, G. B.; Engelking, P. C. Photoelectron Spectroscopy of the CH_3N^- Ion. *J. Chem. Phys.* **1999**, *111* (12), 5349−5360. (b) Wijeratne, N. R.; Fonte, M. D.; Ronemus, A.; Wyss, P. J.; Tahmassebi, D.; Wenthold, P. G. Photoelectron Spectroscopy of Chloro-Substituted Phenylnitrene Anions. *J. Phys. Chem. A* **2009**, *113* (34), 9467−9473.
(33) Wan, H.; Xu, J.; Liu, Q.; Li, H.; Lu, Y.; Abe, M.; Zeng, X. Contrasting Photolytic and Thermal Decomposition of Phenyl Azidoformate: The Curtius Rearrangement Versus Intramolecular C−H Amination. *J. Phys. Chem. A* **2017**, *121* (45), 8604−8613.
(34) Chai, J.-D.; Head-Gordon, M. Systematic Optimization of Long-Range Corrected Hybrid Density Functionals. *J. Chem. Phys.* **2008**, *128* (8), No. 084106.
(35) Weigend, F. Accurate Coulomb-Fitting Basis Sets for H to Rn. *Phys. Chem. Chem. Phys.* **2006**, *8* (9), 1057−1065.
(36) ((a)) Neese, F; Wennmohs, F; Becker, U; Riplinger, C The Orca Quantum Chemistry Program Package. *JPhysChem* **2020**, *152* (22), No. 224108. (b) Schlegel, H. B.; Robb, M. A. Mc Scf Gradient Optimization of the H2c$\vec{o}$H2 + Co Transition Structure. *Chem. Phys. Lett.* **1982**, *93* (1), 43−46.
(37) (a) Hegarty, D.; Robb, M. A. Application of Unitary Group Methods to Configuration Interaction Calculations. *Mol. Phys.* **1979**, *38*, 1795−1812. (b) Eade, R. H. A.; Robb, M. A. Direct Minimization in Mc Scf Theory. The Quasi-Newton Method. *Chem. Phys. Lett.* **1981**, *83*, 362−368. (c) Bernardi, F.; Bottoni, A.; McDouall, J. J. W.; Robb, M. A.; Schlegel, H. B. Mcscf Gradient Calculation of Transition Structures in Organic Reactions. *Farday Symp. Chem. Soc.* **1984**, *19* (0), 137−147. (d) Frisch, M.; Ragazos, I. N.; Robb, M. A.; Schlegel, H. B. An evaluation of three direct MC-SCF procedures. *Chem. Phys. Lett.* **1992**, *189*, 524−528. (e) Yamamoto, N.; Vreven, T.; Robb, M. A.; Frisch, M. J.; Schlegel, H. B. A direct derivative MC-SCF procedure. *Chem. Phys. Lett.* **1996**, *250*, 373−378. (f) Siegbahn, P. E. M. A New Direct CI Method for Large CI Expansions in a Small Orbital Space. *Chem. Phys. Lett.* **1984**, *109* (5), 417−423. (g) Robb, M. A.; Niazi, U. The Unitary Group Approach in Configuration Interaction (CI) Methods. *Comp. Phys. Report* **1984**, *1* (3), 127−236.
(38) Mitsuta, Y.; Asada, T. Curvature-Weighted Nudged Elastic Band Method Using the Riemann Curvature. *J. Comput. Chem.* **2023**, *44* (5), 662−669.
(39) (a) Noorizadeh, S.; Dardab, M. A New NICS-Based Aromaticity Index; NICS-Rate. *Chem. Phys. Lett.* **2010**, *493* (4), 376−380. (b) Krygowski, T. M.; Szatylowicz, H.; Stasyuk, O. A.; Dominikowska, J.; Palusiak, M. Aromaticity from the Viewpoint of Molecular Geometry: Application to Planar Systems. *Chemi. Revi.* **2014**, *114* (12), 6383−6422.
(40) Alonso, M.; Fernández, I.6 - Quantifying Aromaticity According to the Energetic Criterion. In *Aromaticity*, Fernandez, I., Ed.; Elsevier, 2021; pp 195−235.
(41) (a) Govorov, D.; Pitawela, N. R.; Gudmundsdottir, A. D. Aromaticity of the Triplet States of Corannulene and Coronene. *J. Phys. Org. Chem.* **2023**, *36* (1), No. e4464. (b) Li, J.; Rogachev, A. Y. Aromatic Stabilization of Functionalized Corannulene Cations. *Phys. Chem. Chem. Phys.* **2016**, *18* (17), 11781−11791. (c) Steiner, E.; Fowler, P. W.; Jenneskens, L. W. Counter-Rotating Ring Currents in Coronene and Corannulene. *Angew. Chem. Int.Ed.* **2001**, *40* (2), 362−366. (d) Sanyal, S.; Manna, A. K.; Pati, S. K. Functional Corannulene: Diverse Structures, Enhanced Charge Transport, and Tunable Optoelectronic Properties. *ChemPhysChem* **2014**, *15* (5), 885−893.
(42) (a) Stephens, P. J.; Devlin, F. J.; Chabalowski, C. F.; Frisch, M. J. Ab Initio Calculation of Vibrational Absorption and Circular Dichroism Spectra Using Density Functional Force Fields. *J. Phys. Chem.* **1994**, *98* (45), 11623−11627. (b) Krishnan, R.; Binkley, J. S.; Seeger, R.; Pople, J. A. Self-Consistent Molecular Orbital Methods. XX. A Basis Set for Correlated Wave Functions. *J. Chem. Phys.* **1980**, *72* (1), 650−654. (c) Frisch, M. J.; Pople, J. A.; Binkley, J. S. Self-Consistent Molecular Orbital Methods 25. Supplementary Functions for Gaussian Basis Sets. *J. Chem. Phys.* **1984**, *80* (7), 3265−3269.
(43) (a) Herges, R.; Geuenich, D. Delocalization of Electrons in Molecules. *J. Phys. Chem. A* **2001**, *105* (13), 3214−3220. (b) Geuenich, D.; Hess, K.; Köhler, F.; Herges, R. Anisotropy of the Induced Current Density (ACID), a General Method to Quantify and Visualize Electronic Delocalization. *Chem. Rev.* **2005**, *105* (10), 3758−3772.
(44) Keith, T. A.; Bader, R. F. W. Calculation of Magnetic Response Properties Using a Continuous Set of Gauge Transformations. *Chem. Phys. Lett.* **1993**, *210*, 223−231.
(45) Frisch, M. J.; Trucks, G. W.; Schlegel, H. B.; Scuseria, G. E.; Robb, M. A.; Cheeseman, J. R.; Scalmani, G.; Barone, V.; Petersson, G. A.; Nakatsuji, H.; Li, X.; Caricato, M.; Marenich, A. V.; Bloino, J.; Janesko, B. G.; Gomperts, R.; Mennucci, B.; Hratchian, H. P.; Ortiz, J. V.; Izmaylov, A. F.; Sonnenberg, J. L.; Williams-Young, D.; Ding, F.; Lipparini, F.; Egidi, F.; Goings, J.; Peng, B.; Petrone, A.; Henderson, T.; Ranasinghe, D.; Zakrzewski, V. G.; Gao, J.; Rega, N.; Zheng, G.; Liang, W.; Hada, M.; Ehara, M.; Toyota, K.; Fukuda, R.; Hasegawa, J.; Ishida, M.; Nakajima, T.; Honda, Y.; Kitao, O.; Nakai, H.; Vreven, T.; Throssell, K.; Montgomery, J. A., Jr.; Peralta, J. E.; Ogliaro, F.; Bearpark, M. J.; Heyd, J. J.; Brothers, E. N.; Kudin, K. N.; Staroverov, V. N.; Keith, T. A.; Kobayashi, R.; Normand, J.; Raghavachari, K.; Rendell, A. P.; Burant, J. C.; Iyengar, S. S.; Tomasi, J.; Cossi, M.; Millam, J. M.; Klene, M.; Adamo, C.; Cammi, R.; Ochterski, J. W.;

https://doi.org/10.1021/jacs.4c07846
J. Am. Chem. Soc. XXXX, XXX, XXX−XXX

Martin, R. L.; Morokuma, K.; Farkas, O.; Foresman, J. B.; Fox, D. J. *Gaussian 16, Revision C.01*; Gaussian, Inc.: Wallingford, CT, 2016.
(46) Baird, N. C. Quantum Organic Photochemistry. II. Resonance and Aromaticity in the Lowest $3\pi,\pi^*$ State of Cyclic Hydrocarbons. *J. Am. Chem. Soc.* **1972**, *94* (14), 4941−4948.

https://doi.org/10.1021/jacs.4c07846
J. Am. Chem. Soc. XXXX, XXX, XXX−XXX